Peer-reviewed version available at Remote Sens. 2018, 10, 1690; doi:10.3390/rs10111690

Article

Deep Learning with unsupervised data labeling for weeds detection on UAV images

M Dian Bah [1], Adel Hafiane [2,*] and Raphael Canals [1]

[1] Univ. Orleans, PRISME, EA 4229, F45072, Orleans, France; m-dian.bah@univ-orleans.fr; raphael.canals@univ-orleans.fr
[2] INSA-CVL, PRISME, EA 4229, F18020, Bourges, France; adel.hafiane@insa-cvl.fr
* Correspondence: adel.hafiane@insa-cvl.fr

Version September 5, 2018 submitted to Preprints

Abstract: In recent years, weeds is responsible for most of the agricultural yield losses. To deal with this threat, farmers resort to spraying pesticides throughout the field. Such method not only requires huge quantities of herbicides but impact environment and humans health. One way to reduce the cost and environmental impact is to allocate the right doses of herbicide at the right place and at the right time (Precision Agriculture). Nowadays, Unmanned Aerial Vehicle (UAV) is becoming an interesting acquisition system for weeds localization and management due to its ability to obtain the images of the entire agricultural field with a very high spatial resolution and at low cost. Despite the important advances in UAV acquisition systems, automatic weeds detection remains a challenging problem because of its strong similarity with the crops. Recently Deep Learning approach has shown impressive results in different complex classification problem. However, this approach needs a certain amount of training data but, creating large agricultural datasets with pixel-level annotations by expert is an extremely time consuming task. In this paper, we propose a novel fully automatic learning method using Convolutional Neuronal Networks (CNNs) with unsupervised training dataset collection for weeds detection from UAV images. The proposed method consists in three main phases. First we automatically detect the crop lines and using them to identify the interline weeds. In the second phase, interline weeds are used to constitute the training dataset. Finally, we performed CNNs on this dataset to build a model able to detect the crop and weeds in the images. The results obtained are comparable to the traditional supervised training data labeling. The accuracy gaps are 1.5% in the spinach field and 6% in the bean field.

Keywords: Weeds detection, Deep learning, Unmanned aerial vehicle, Image processing, Precision agriculture, Crop lines detection

1. Introduction

Currently, losses due to pests, diseases and weeds can reach 40% of global crop yields each year and this percentage is expected to increase significantly in the coming years [1]. The usual weeds control practices consist in spraying herbicides all over the agricultural field. Those practices involve significant wastes and costs of herbicides for farmers and environmental pollution [2]. In order to reduce the amount of chemicals while continuing to increase productivity, the concept of precision agriculture was introduced [3,4]. Precision agriculture is defined as the application of technology for the purpose of improving crop performance and environmental quality [3]. The main goal of precision agriculture is to allocate the right doses of input at the right place and at the right time. Weeds detection and characterization represent one of the major challenges of the precision agriculture.

In the literature several methods of detection of weeds are proposed with different acquisition system. Compared to robot or satellite acquisitions, drones have been considered more efficient since they allow a fast acquisition of the field with very high spatial resolution and low cost [5,6]. Despite the important advances in UAV acquisition systems, the automatic detection of weeds remains a challenging problem. In recent years, deep learning techniques have shown a dramatic improvement

for many computer vision tasks, but still not widely used in agriculture domain. Indeed recent development showed the importance of these techniques for weeds detection [7,8]. However, the huge quantities of the data required in the learning phase, have accentuated the problem of the manual annotation of these datasets. The same problem rises in agriculture data, where labeling plants in a field image is very time consuming. So far, very little attention have been payed to the unsupervised annotation of the data to train the deep learning models, particularly for agriculture.

In this paper, we propose a new fully automatic learning method using Convolutional Neuronal Networks (CNNs) with unsupervised training set labeling for weeds detection on UAV images. This method is performed in three main phases. First we automatically detect the crop lines and using them to identify the interline weeds. In the second phase interline weeds are used to constitute our training dataset. Finally, we performed CNNs on this database to build a model able to detect the crop and weeds in the images.

This paper is divided into five parts. In the section 2 we discuss the related work. Section 3 presents the proposed method. In section 4 we comment and discuss the experimental results obtained. Section 5 concludes the paper.

2. Related work

In literature, several approaches have been used to detect weeds with different acquisition systems. The main approach for weeds detection is to extract vegetation from the image using a segmentation and then discriminate crop and weeds. Common segmentation approaches use color and multispectral information, to separate vegetation and background (soil and residues). Specific indices are calculated from these information to effectively segment vegetation [9].

However, weeds and crop are hard to discriminate by using spectral information because of their strong similarity. Regional approaches and spatial arrangement of pixels are preferred in most cases. In [10], Excess Green Vegetation Index (ExG) [11] and the Otsu's thresholding [12] have helped to remove background (soil, residues) before to perform a double Hough transform [13] in order to identify the main crop lines in perspective images. Then, to discriminate crop and weeds in the segmented image, the authors applied a region-based segmentation method developing a blob coloring analysis. Thus any region with at least one pixel belonging to the detected lines is considered to be crop, otherwise it is weeds. Unfortunately, this technique failed to handle weeds close to crop region. In [14] an object-based image analysis (OBIA) procedure was developed on series of UAV images for automatic discrimination of crop rows and weeds in maize field. For that, they segmented the UAV images into homogeneous multi-pixel objects using the multi-scale algorithm [15]. Thus, the large scale highlights structures of crop lines and the small scale brings out objects that lie within crop lines. They have found that the process is strongly affected by the presence of weed plants very close or within the crop rows.

In [16], 2-D Gabor filters have been applied to extract the features and Artificial Neural Network (ANN) for broadleaf and grass weeds classification. Their results showed that joint space-frequency texture features have potential for weed classification. In [17], the authors rely on morphological variation and use neural network analysis to separate weeds from maize crop. Support Vector Machine (SVM) and shape features was suggested for the effective classification of crops and weeds in digital images in [18]. On their experiment, a total of fourteen features that characterize crops and weeds in images were tested to find the optimal combination of features which provides the highest classification rate. [19] suggested that in the image, edge frequencies and veins of both the crop and the weed have different density properties (strong and weak edges) to separate crop from weed. A semi-supervised method has been proposed in [20] to discriminate weeds and crop. The Ostu thresholding was applied twice on ExG. In first step, authors used segmentation to remove the background then, in the second one they create two classes supposed to be crop and weeds. K-means clustering was used to select one hundred samples of each class for the training. SVM classifier with geometric features, spatial features, first and second-order statistics was extracted on the red, blue, green and ExG bands. The

method has proven to be effective in sunflower field, but less robust in the corn field because of shade produced by corn plants. In [21], authors used texture features extracted from wavelet sub-images to detect and characterize four types of weeds in a sugar beet field. Neural networks have been applied as classifier. The use of wavelets proved to be efficient for the detection of weeds even at a stage of growth of beet greater than 6 leaves. [22] evaluate weeds detection with support vector machine and artificial neural networks in four species of common weeds in sugar beet fields using shape features. In [23] a semi-automatic Object-Based Image Analysis (OBIA) procedure have been developed with Random Forests (RF) combined with feature selection techniques to classify soil, weeds and maize. With all these articles, we can notice that the selected features change in general from one type of culture to another or from one type of data to another.

Recently, convolutional neural networks have emerged as a powerful approach for computer vision tasks. CNNs [24] progressed mostly through the success of this method in ImageNet Large Scale Vision Recognition Challenge 2012 (ILSCVR12) and the creation of AlexNet network in 2012 which showed that a large, deep convolutional neural network is capable of achieving record-breaking results on a highly challenging dataset using purely supervised training [25]. Nowadays deep learning is applied in several domains to help solve many big data problems such as computer vision, speech recognition, and natural language processing. In agriculture domain, CNNs are applied to classify patches of water hyacinth, serrated tussock and tropical soda apple in [26]. [27] used CNNs for semantic segmentation in the context of mixed crops on images of an oil radish plot trial with barley, grass, weed, stump and soil. [28] provide accurate weeds classification in real sugar beet fields with mobile agricultural robots. [7] applied AlexNet for the detection of weeds in soybean crops. In [8] AlexNet is applied for weeds detection in different crop fields such as the beet, spinach and bean in UAV imagery.

The main common point between the supervised machine learning algorithms is the need of training data. For a good optimization of deep learning models it is necessary to have a certain amount of labeled data. But as mentioned before creating large agricultural datasets with pixel-level annotations is an extremely time consuming task. Little attempts have been made to develop fully automatic system for training and identification of weeds in agricultural fields. In a Recent work, [29] suggest the use of synthetic training datasets. However, this technique requires a precise modeling in terms of texture, 3D models and light conditions. [30] an automatic image processing has been developed to discriminate between crop and weed pixels combining spatial and spectral information extracted from four-band multispectral images. Image data was captured at 3 m above ground, with a camera mounted on a pole kept manually. The spatial approach (Hough Transform) is used to detect crop rows and to build a training dataset. SVM is applied to the spectral information to make classification. This method assumes weeds and crops have different spectral information and that is not always the case in agricultural fields. The success of this kind of method lies on better features selection which involves a human analysis according to the agriculture field. To the best of our knowledge there is no work for weeds detection on UAV images using automatic labeling of training images and deep learning.

3. Proposed Method

In modern agriculture, most of crops are grown in regular rows separated by a defined space that depends on type of the crop. Generally, plants that grow out of the rows are considered as weeds commonly referred as inter-line weeds. Several studies have used this assumption to locate weeds using the geometric properties of the rows [31]. The main advantage of such technique is that it is unsupervised and does not depend on the training data. Indeed, based on this hypothesis we detect first the crop rows, then inter-line vegetation is used to constitute our training database which is categorized into two classes crop and weed. Thereafter, we performed CNNs on this database to build a model able to detect the crop and weeds in the images. The flowchart (Figure 1) depicts the main steps of the proposed method. Next sections describes in details each step.

Peer-reviewed version available at Remote Sens. 2018, 10, 1690; doi:10.3390/rs10111690

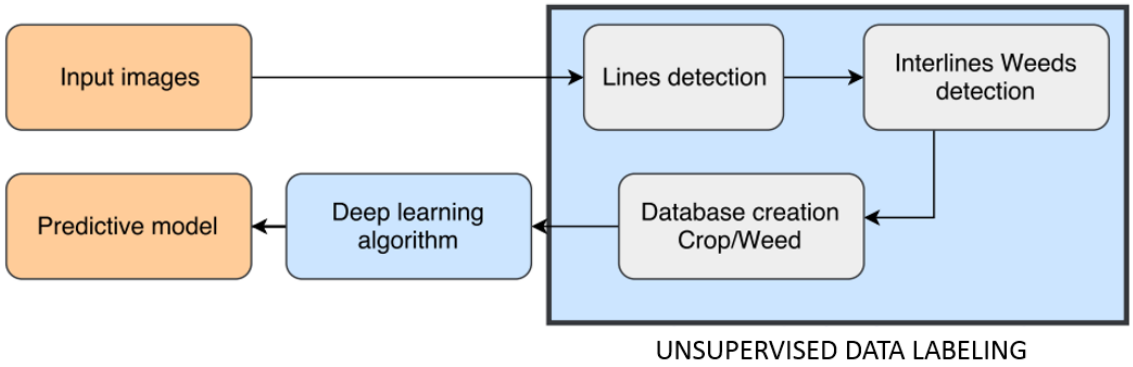

Figure 1. Flowchart of the proposed method

3.1. Crop lines detection

A crop row can be defined as a composition of several parallel lines. The aim is to detect the main line of each crop row. For that purpose we have used a Hough transform to highlight the alignments of the pixels. In Hough space there is one cell by line which involve an aggregation of cells by crop row. The main lines in Hough space correspond to the cells which contains the maximum of vote (peak) on each aggregation. Before starting any line detection procedure, generally pre-processing is required to remove undesirable perturbations such as shadows, soil or stones. Here we have used the ExG (Eq. 1) with the Otsu adaptive thresholding to discriminate between vegetation and background.

$$ExG = 2g - r - b \tag{1}$$

where r, g and b are the normalized RGB coordinates.

Hough transform is one of the most widely used methods for lines detection and it is often integrated in tools for guiding agricultural machines because of its robustness and ability to adjust discontinuous lines caused by missing crop plants in the row or poor germination [32]. Usually, for crop lines detection, Hough transform is directly applied to the segmented image. This procedure is computational expensive and depends on the density of the vegetation in crop rows and there is also a risk of the lines over-detection. We have addressed this problem by using the skeleton of each row, this approach has shown better performances in (Bah et al. 2017). The skeleton provided a good overall representation of the structure of the field, namely orientations and periodicity. Indeed, the Hough transform $H(\theta, \rho)$ is computed on the skeleton with a θ resolution equal to 0.1° letting θ take values in the range of $]-90^\circ; 90^\circ]$ and ρ resolution equal to 1. Thanks to a histogram of the skeletons directions, the most represented angle is chosen as the main orientation θ_{lines} of crop lines. $H(\theta, \rho)$ has been normalized $H_{norm}(\theta, \rho)$ in order to give the same weight to all the crop lines, especially the short ones close to the borders of the image [10]. $H_{norm}(\theta, \rho)$ is defined as the ratio between the accumulator of the vegetation image and the accumulator of a totally white image of the same size $H_{ones}(\theta, \rho)$. To disregard the small lines created by aggregation of weeds in inter-row a threshold of 0.1 was applied to the normalized Hough transform. Moreover in modern agriculture crops are usually sown in parallel lines with the same interline distance that is the main peaks corresponding to the crop lines are aligned around an angle in the Hough space with same gaps. Unfortunately, because of the realities in the agricultural field the lines are not perfectly parallel, thus the peaks in the Hough space have close but different angles and the interline distance is not constant. In order to not skip any crop line during the detection, all the lines which have in Hough space a peak whose angle compared to the overall orientation (θ_{lines}) of the lines does not exceed 20° are retained. Figure 2 presents the flowchart of the lines detection method. However, to avoid detecting more than one peak in an aggregation (reduce over-detection), every time that we identify a peak of a crop row in $H_{norm}(\theta, \rho)$, we identify the

Preprints (www.preprints.org) | NOT PEER-REVIEWED | Posted: 5 September 2018 doi:10.20944/preprints201809.0088.v1

Peer-reviewed version available at Remote Sens. 2018, 10, 1690; doi:10.3390/rs10111690

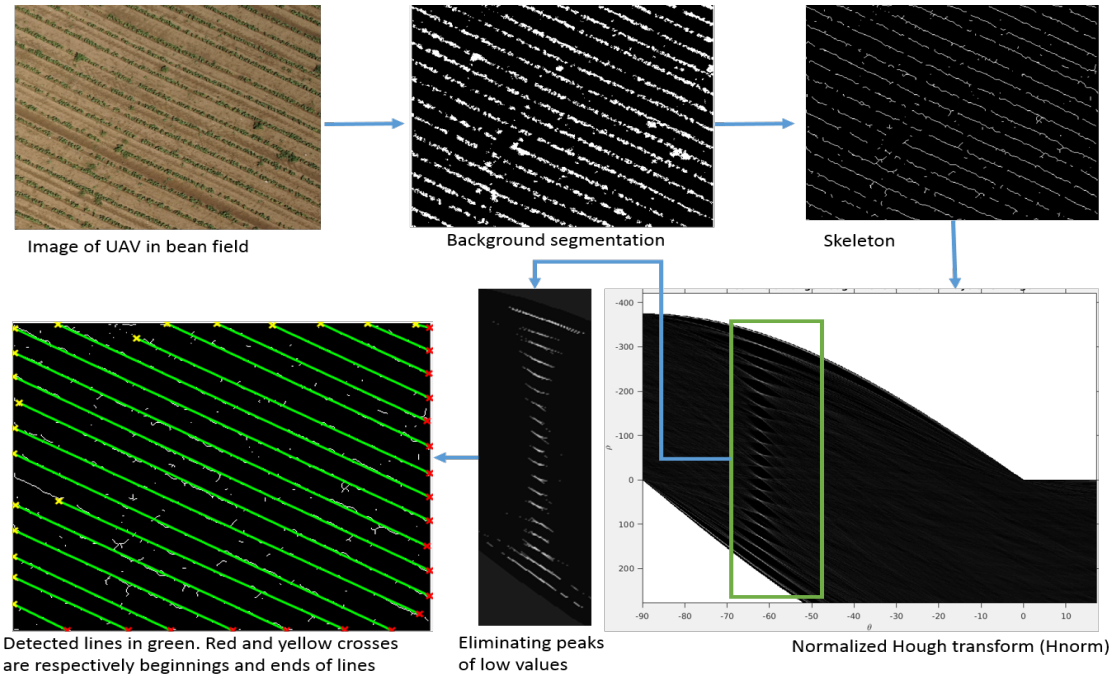

Figure 2. Flowchart of crop lines detection method.

corresponding skeleton, and then we delete the votes of this skeleton in $H_{norm}(\theta,\rho)$ before continuing. All the steps are summarized in algorithm 1.

Algorithm 1: Crop lines detection.

input : skeletons
output: crop lines

Computation of the skeletons angle
Computation of the main orientation θ_{lines} of the crop lines
Hough transform of the skeletons $H(\theta,\rho)$
$H_{norm}(\theta,\rho)$=$H(\theta,\rho)$/Hones(θ,ρ)
while *maximum of* $H_{norm}(\theta,\rho) > 0.1$ **do**
    Computation of the maximum of $H_{norm}(\theta,\rho)$ and the corresponding angle θ_m
    Recovery of the line corresponding to the maximum ($Line_{skeleton}$)
    Computation of the normalized Hough transform ($H_{temp}(\theta,\rho)$) of the $Line_{skeleton}$
    $H_{norm}(\theta,\rho)$=$H_{norm}(\theta,\rho) - H_{temp}(\theta,\rho)$
    if $\theta_m > \theta_{lines} - 20°$ *and* $\theta_m < \theta_{lines} + 20°$ **then**
        The detected line is a crop line

3.2. Unsupervised training data labeling

The unsupervised training dataset annotation is based on the detected lines obtained in previous section. According to hypothesis that the lines detected are mainly at the center of the crop rows (Figure 3) we performed a mask to delimit the crop rows. Hence, the vegetation overlapped by the mask correspond to the crop. This mask is obtained from the intersection of superpixels formed by the simple linear iterative clustering (SLIC) algorithm [33] and the detected lines. SLIC is chosen since it is simple and efficient in terms of results quality and computation time. It is an adaptation of k-means for superpixels generation with a control on size and compactness of superpixels. SLIC creates a local grouping of pixels based on their spectral values defined by the values of the CIELAB color space and

Peer-reviewed version available at Remote Sens. 2018, 10, 1690; doi:10.3390/rs10111690

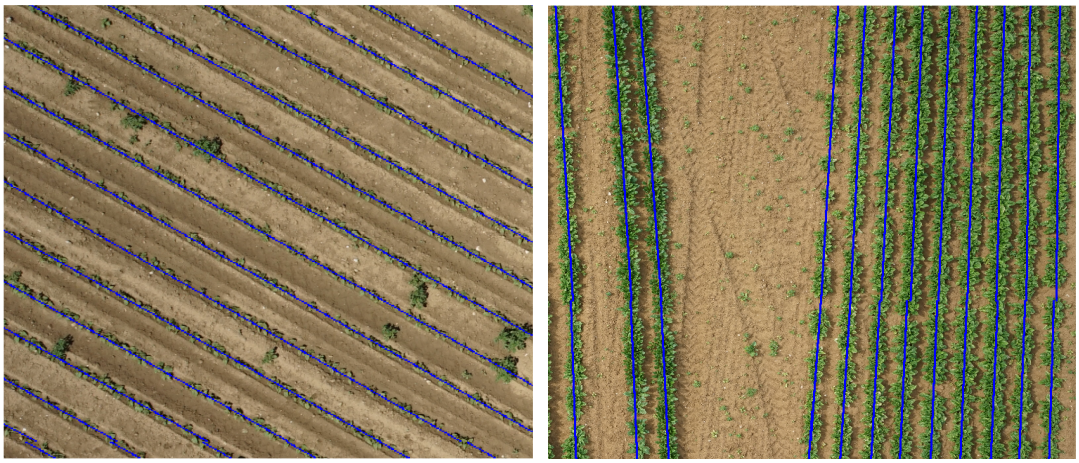

(a) (b)

Figure 3. From left to right lines detection in bean (a) and spinach (b) fields. Detected lines are in blue. In the spinach field interline distance and the crop rows orientation are not regular. The detected lines are mainly in the center of the crop rows.

their spatial proximity. A higher value of compactness makes superpixels more regularly shaped. A lower value makes superpixels adhere to boundaries better, making them irregularly shaped. Since here the goal is to create a mask around the detected crop lines able to delimit the crop rows we have chosen a compactness of 20 because we found it was less sensitive to the variation of color caused by the effect of light and shadow. Figure 4 shows examples of images segmented with different size of superpixels.

Once the crop is identified, next step consists in detection of the interlines weeds. Interline weed is plant which grows up in the interline crop. To detect weeds that lie in inter-row we performed a blob coloring algorithm. Hence any region that does not intersect with the crop mask is regarded as weed. Besides, vegetation pixels which do not belong to the crop mask neither to the interlines weeds are attributed to the potential weeds. Figure 5 shows the mask of crop, interline weeds and potential weeds. To construct the training dataset, we extracted patches from the original images using positions of the detected inter-row weeds and crops. For weeds samples we performed bounding boxes on each segmented intra-row weed. For the crop samples, sliding window has been applied on the input image using positions relative to the segmented crop lines. Thus, for a given position of the window if it intersects the binary mask and there is no inter-lines weeds pixels we attribute it to the crop class. Generally, the crop class has much more samples than the weed. In the case that we have less interline weeds samples and in the same time we have a wide potential weeds as in Figure 5 we propose to collect samples from the potential weeds. Hence, the window which contains only potential weeds is labeled as weeds. Windows which contain crop and potential weeds, where we have more potential weeds than crop are not retained.

3.3. Crop/Weeds classification using Convolutional Neural Networks

CNNs are a part of Deep learning approach, they showed impressive performances in many computer vision tasks [34]. CNNs are made up of two types of layers, the convolutional layers which extract different characteristics of images and the fully connected layers based on multilayer perceptron. The number of convolutional layers depends on the classification task and also the number and the size of the training data.

In this work we used a Residual Network (ResNet), this network architecture was introduced in 2015 [35]. It won the ImageNet Large Scale Vision Recognition Challenge 2015 with 152 layers.

Preprints (www.preprints.org) | NOT PEER-REVIEWED | Posted: 5 September 2018 doi:10.20944/preprints201809.0088.v1

Peer-reviewed version available at Remote Sens. 2018, 10, 1690; doi:10.3390/rs10111690

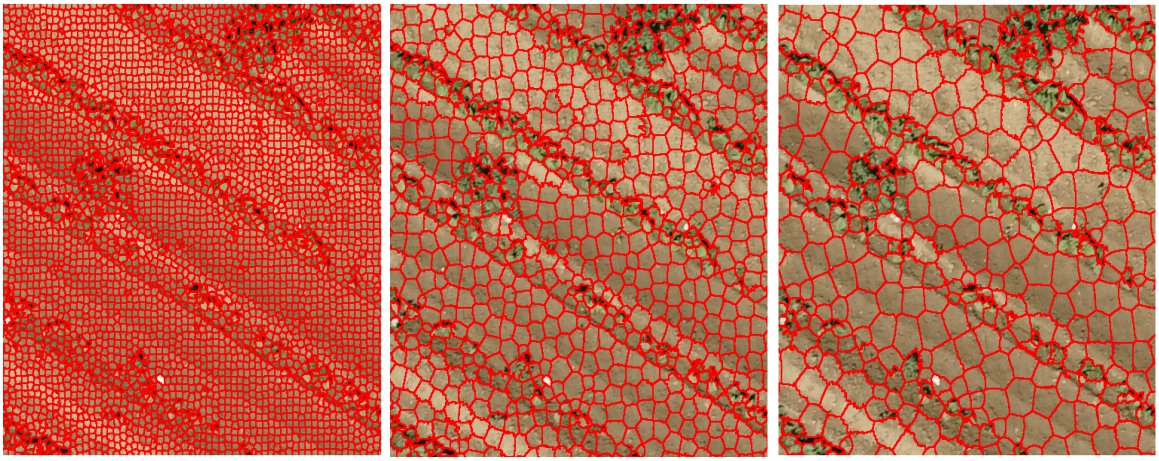

(a) (b) (c)

Figure 4. Examples of superpixels computed on images of dimensions N=7360×4912. From left to right, the image is segmented with a number of superpixels equal to 0.5% × N, 0.1%×N and 0.01% ×N respectively.

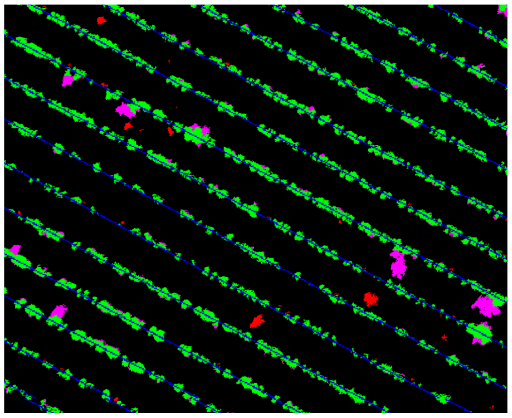

Figure 5. Detection of interline weeds (red) after lines detection (blue) in a bean image. The mask of crop is represented in green and the potential weeds in magenta.

However, according to the size of data we used the ResNet with 18 layers (ResNet18) described in [35] because it has shown a better result than AlexNet and VGG13 [36] in the ImageNet challenge. Due to abundant categories and significant number of images in ImageNet, studies revealed the performance of transferability of networks trained with ImageNet dataset. Thus we performed fine tuning to train the networks in our data. Fine-tuning means that we start with the learned features on the ImageNet dataset, we truncate the last layer (softmax layer) of the pre-trained network and replace it with new softmax layer that are relevant to our own problem. Here the thousand categories of ImageNet have been replaced by two categories (crop and weeds).

3.4. Features Extraction

Although color indices do make sense in distinguishing between the vegetation and the background, they become less effective when applied to classify the species of plants. Sometimes, the color of weeds and crop leaves look almost the same. Moreover, the result will become unreliable under different lighting conditions. To solve this problem, several features have been proposed. We compute series of statistics features, shape features and texture features which have been selected

on other works [19–21,37]. A procedure of feature selection is then used to analyze the most suitable features.

3.4.1. Color features

The color features used are: mean and standard deviation of three bands of the RGB image and ExG image. In order to make the color features consistent with different lighting levels every color bands was normalized by the sum of all the three color bands.

3.4.2. Geometric shape feature

Based on [18], three parameters namely Form Factor, Elongatedness and Solidity have been computed as geometric features. We named the vector of feature created by those three as *Geo*3.

$$FormFactor = \frac{4 * \pi * area}{perimeter^2}$$

$$Elongatedness = \frac{area}{thickness^2}$$

$$Solidity = \frac{area}{convex_{area}}$$

Here, area is defined as the number of pixels with a value '1' in the binary image. Perimeter is defined as the number of pixels with a value '1' for which at least one of the eight neighboring pixels has the value '0', implying that perimeter is the number of border pixels. Convex area is the area of the smallest convex hull that covers all the plant pixels in an image.

3.4.3. Edge density

Edge detection is a method of image segmentation which uses the fact that the edge frequencies and veins of both the crop and the weed have different density properties (strong and weak edges) to separate crop from weed [19]. In the follow of this article we will denote edge density as *Edensity*. It is defined as:

$$ED = \frac{edge_{area}}{area}$$

Here, area is defined as the number of pixels with a value '1' in the binary image. The image will then be computed by Sobel edge detection method, all the pixels marked as edge in the binary edge image will be added together, the sum of them is the $edge_{area}$.

3.4.4. HOG

Contour attributes generally correspond to the histogram of the gradient orientation. HOG [38] is fast comparing to the SIFT (because no smoothing is computed), It is computed on a large number of cells uniformly spaced image and overlapping. Thanks to the normalization of the local contrast, it is invariant to the conditions of illumination. HOG has been initially used for pedestrian detection, but it has shown robustness in many other issues. In 2010, Xiao et *al.* introduced HOG to identify plant leaves [39]. That experiment is inspiring and indicates that we can combine the features extracted by HOG methods to realize leaves classification.

3.4.5. Haralick texture

The co-occurrence matrix makes possible to obtain the occurrence frequency of a pattern of 2 pixels separated by a distance d along a direction θ. In [40] authors propose 14 features that can be computed on this matrix. These features have the aim of highlighting the visual characteristics, statistics, the randomness of the distribution of the gray levels and the linear dependence of the gray levels on a neighborhood of pixels (the homogeneity, the coarseness, the periodicity, the smoothness, ...).

In 2012, Haralick method have been applied to extract texture features in classification of plants species [41]. The authors used 6 of the Haralick features, including: autocorrelation, contrast, correlation, dissimilarity, energy and entropy. Same features are used here and they are called Haralick features.

3.4.6. Gabor wavelets

This method realizes joint space-frequency analysis.The short time Fourier transform with a Gaussian window is called the Gabor transform. It is able to preserve both local and global information in image. In 2003, Tang et *al.* fixed the filter orientation at 90° for the classification of broad and narrow leave [16]. By analyzing the separation between classes of each feature, they concluded that a filter bank with four frequency levels from 4 to 7 are suitable for the classification task. Therefore, we have chosen from 4 to 7 as the frequencies, while 0°, 45° and 90° to be the orientation. We generated 12 Gabor features.

3.5. SVM or Support Vector Machine

The ideal for a good classification is to have a fast classifier, which avoids overfitting, able to respond to multi-class problems, to separate classes with a large gap or margin, to manage large features vector. In this paper we applied the SVM or Support Vector Machine or Large Margin Separator. It is one of the most successful machine learning methods. Its popularity stems from the fact that it ensures a separation of classes with a very great difference if it is provided with two-class data and also because it is adapted to linear and nonlinear cases.

3.6. Random Forest (RF)

The Random Forest, is a meta-classier, It combines several weak classifiers to form a strong classifier. RF easily handles multi-class problems and is robust to large features and has a very low risk of overfitting. It is used in several applications such as point tracking in video surveillance, medical imaging, for games in Microsoft's Kinect. In addition, the RF has been shown to be ideally suited for classifying high resolution UAV data [42]. It is structured like a real forest with trees, where each tree has roots, branches and leaves. The trees correspond to the different classifiers, the first node corresponds to the root of the tree (the point of entry of our data), each node is then separated into intermediate nodes and each leaf corresponds to a terminal node where the final decision is stored. The trees of the forest are built using bagging or Bootstrap aggregating. The principle of bagging is to construct each tree by selecting a subset of n observations among the N learning data ($n < N$) obtained by random sampling with delivery. The objective is to get the trees as different as possible, in other words to obtain uncorrelated trees because the more the trees are different, the more robust the forest is. The other advantage of bagging is that it makes possible to estimate the prediction error of the forest by using "out-of-bag" (OOB) or data not used during the construction of the trees.

4. Experiments and results

Experiments were conducted on two different fields of bean and spinach (Figure 6). The images are acquired by a DJI Phantom 3 Pro drone that embeds a 36 megapixel (MP) RGB camera at an altitude of 20 m. This acquisition system enables to obtain very high resolution images with a spatial resolution about 0.35 cm.

To build the unsupervised training database, we selected two different parts of given field. The first one (Part1) is used to collect the training data and the other (Part2) for test data collection.

To create the crop binary mask after line detection the superpixels compactness have been set to 20 and the number of superpixels is equal to 0.1%×N, where N=7360×4912 (Figure 4b). In this experiments, we used a 64 by 64 window to create the weed and crop training databases. This window size provides a good trade off between plant type and overall information. A small window is not sufficient to capture whole plant and can lead to confuse culture and non culture, because in some conditions crop and weed leaves have the same visual characteristics. In other hand, too large size

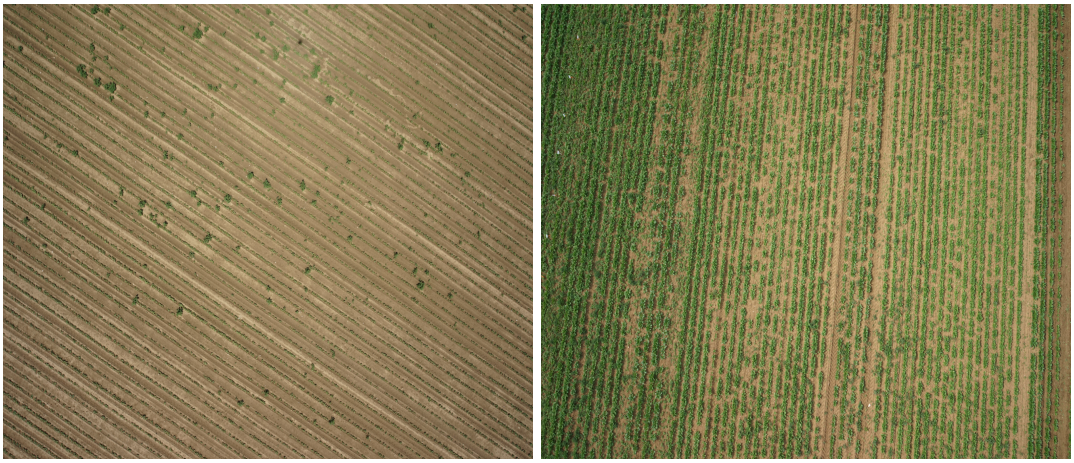

(a) (b)

Figure 6. Example of images taken in the bean (a) and spinach fields (b). The bean field has less interline weeds and is predominately composed of potential weeds. The inter-row distance is stable and the plant is sparse compared to the spinach field which presents a dense vegetation in the crop rows and irregular inter-row distance. Spinach field has more interlines weeds and it has few potential weeds.

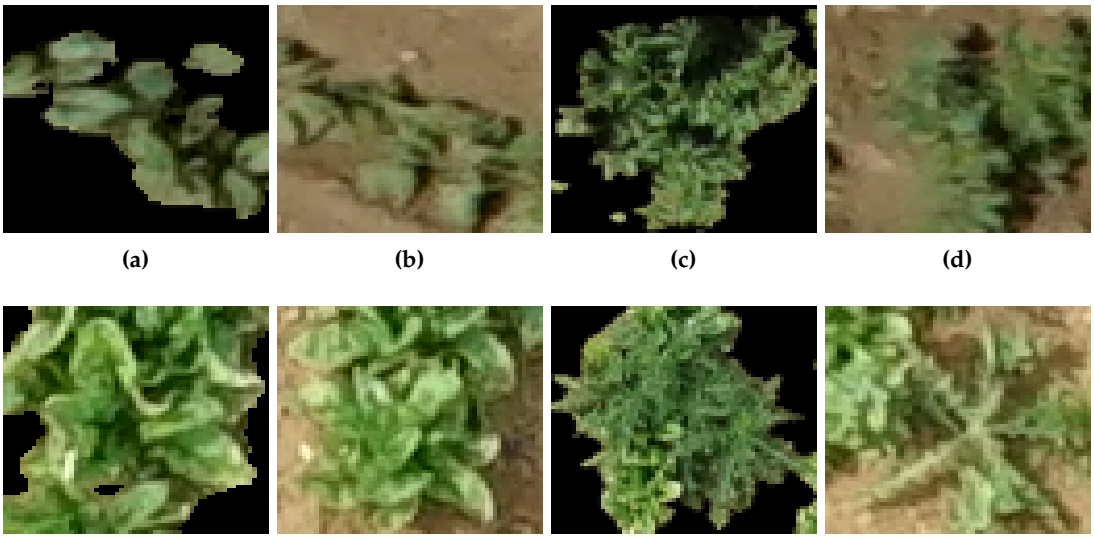

(a) (b) (c) (d)

(e) (f) (g) (h)

Figure 7. Example of crop and weed samples of size 64×64 with and without background. Bean: samples of crop (a and b), samples of weed. (c and d). Spinach: samples of crop (e and f) and samples of weed (g and h). Depending on the size of the plant and the position of the window we obtain a plant or aggregation of plants per window.

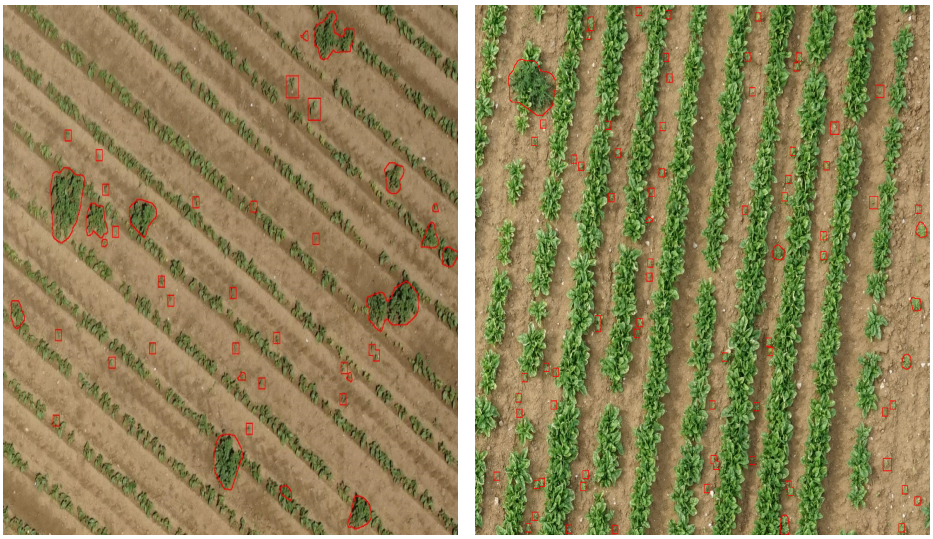

(a) (b)

Figure 8. Parts of bean field (a) and spinach field (b) with the weeds labeled manually by an expert in red. The manual labeling has taken about 2 working days.

Table 1. Training and validation data in the bean field.

Data	Class	Training	Validation	Total
Supervised	Crop	17192	11694	28886
labeling	Weed	17076	9060	16136
Total		34868	20754	45022
Unsupervised	Crop	7688	1928	9616
labeling	Weed	5935	1493	7428
Total		13623	3421	17044

presents a risk of having crop and weeds in the same window. In the bean field, the weeds present are thistles and young sprouts of potato from previous sowing on the same field. This field has few interline weeds so we have decided to include the potential weeds in weeds samples. After applying the unsupervised labeling method, the number of samples collected is 673 for weeds and 4861 for crops. Even with potential weeds the collected samples was unbalanced. To address this problem we realized data-augmentation. Hence we have performed two contrast changes, a smoothing with a Gaussian filter and three rotations (90°, 180°, 270°). The strong heterogeneity in the fields can often be encountered from one part of the field to another. This heterogeneity may be a difference of soil moisture, presence of straw, etc... In order to make our models robust to the background, we mixed samples with background and no background. Samples without background were obtained by applying ExG followed by Otsu's thresholding on previously created samples (see Figure 7). We evaluated the performance of our method by comparing models created by data labeled in supervised and unsupervised way.

The supervised training dataset were labeled by human experts. A mask is performed manually on the pixels of weeds and crops. Figure 8 presents weeds manually delineated by an expert in red. The supervised data collected were also unbalanced so we have carried out the same data augmentation procedure performed on the unsupervised data. The total number of samples is shown in the Table 1.

The spinach field is more infected than the bean field, there are mainly thistles. In total 4303 samples of crop and 3626 samples of weed were labeled in unsupervised way. Unlike bean field

Table 2. Training and validation data in the spinach field.

Data	Class	Training	Validation	Total
Supervised	Crop	11350	2838	14188
labeling	Weed	8234	2058	10292
Total		19584	4896	34772
Unsupervised	Crop	6884	1722	8606
labeling	Weed	5800	1452	7252
Total		12684	3174	15858

we have obtained a less unbalanced data. Therefore, the only data augmentation applied is adding samples without background. The same processing has been applied on the supervised data. Table 2 presents the number of samples.

4.1. Evaluation of ResNet results

After the creation of both weed and crop classes, 80% of samples were selected randomly for the training, and the remaining ones were used for validation. The Tables 1 and 2 present the training and validation data performed on each field. For finetuning we tested different values of the learning rate. The initial learning rate is set to 0.01 and updated every 200 epochs. The update is done by dividing the learning rate by factor of 10. Figure 9 shows the evolution of the loss function during training for supervised and unsupervised datasets for spinach and bean fields. From these figures we can notice that the validation loss curves decrease during about the first 80 epochs before to increase and to converge (behavior close to overfitting phenomenon). This overfitting phenomenon is less emphasized in the supervised labeled data of bean. The best models were obtained during the first learning phase with a learning rate of 0.01.

Performance of models have been evaluated on test ground truth data collected in Part2 by supervised way on each field, the Table 3 presents the samples. The performance of the classification results are illustrated with Receiver Operating Characteristic (ROC) curves.

Table 3. Number of test samples used for each field.

Field	Samples of crop	Sample of weed
Bean	2139	1852
Spinach	1523	1825

From the ROC curves (Figure 10) we can notice that the AUC (Area Under the Curve) are close to or greater than 90%. Although both types of learning data provide good results and their results are comparable. On both fields we remark that positive rate of 20% provides a true positive rate greater than 80%. The differences of performance between supervised and unsupervised data labeling are about 6% in the bean field and about 1.5% in the spinach field. The performance gap in the bean field can be explained by the low presence of weeds in the inter-row.

Both fields are infested mainly by thistles, we tested the robustness of our models by exchanging the samples of weeds from the bean field with that of the spinach field.

In Figure 11 the results obtained show that despite the small samples harvested in the bean filed, those data are suitable to the spinach field and the model created with unsupervised labeling in the spinach field is most sensitive to the presence of young potato sprouts among bean weed samples.

Preprints (www.preprints.org) | NOT PEER-REVIEWED | Posted: 5 September 2018 doi:10.20944/preprints201809.0088.v1

Peer-reviewed version available at Remote Sens. 2018, 10, 1690; doi:10.3390/rs10111690

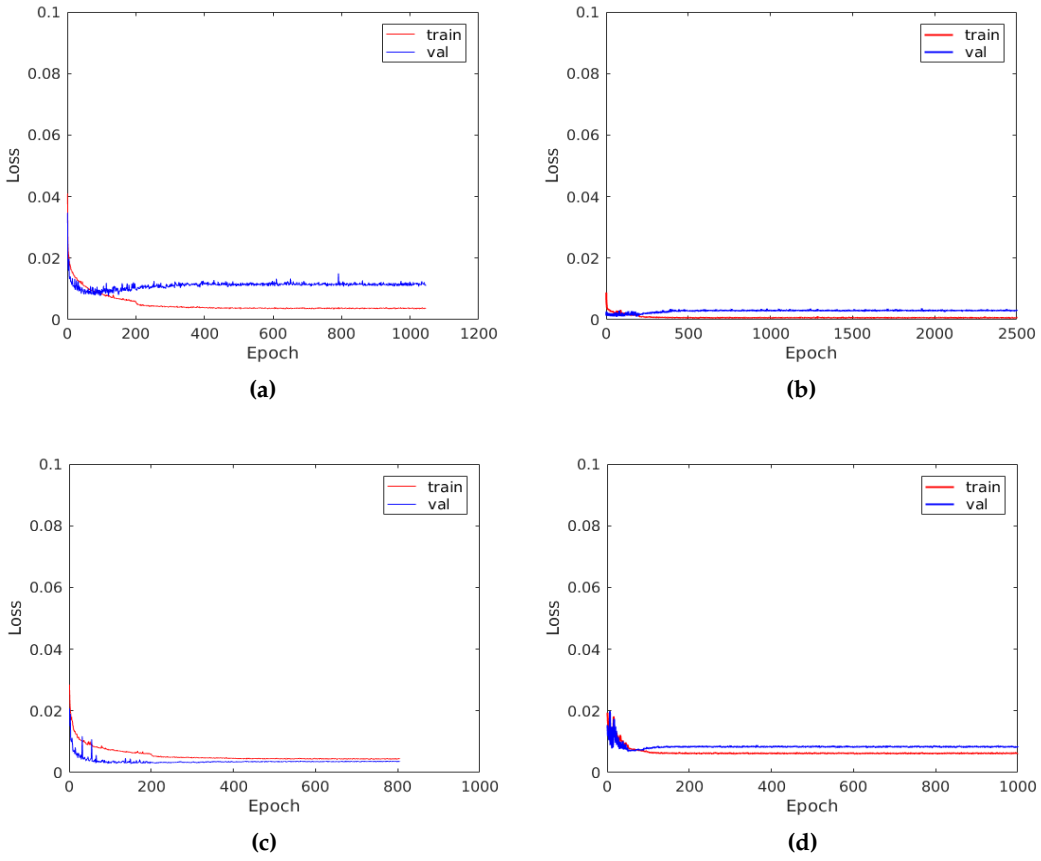

Figure 9. Evolution of the loss during training for supervised and unsupervised data in the fields of spinach and bean. The validation loss curves decrease during about the first 80 epochs before to increase and converging. First line represents the spinach field and the second one the bean field. The first and second column are respectively the training on the the supervised and unsupervised data.

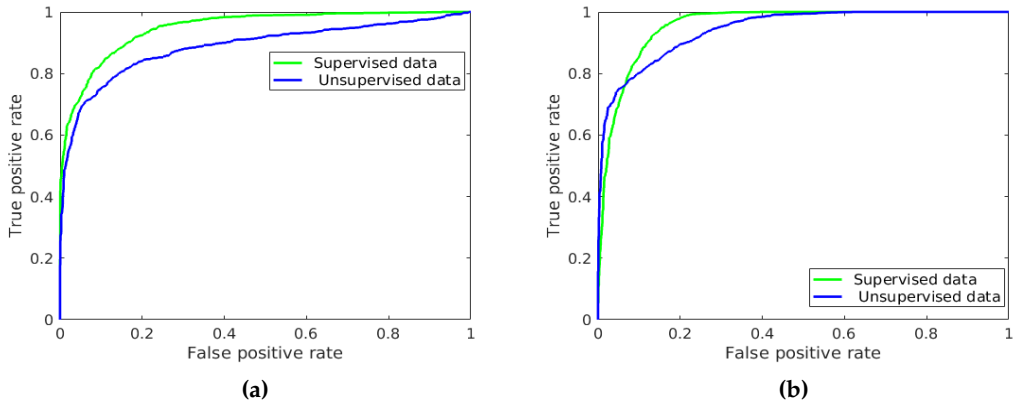

Figure 10. ROC curves of the test data with the unsupervised and supervised data labeling.From left to right the ROC curves computed on the bean (a) and spinach (b) test data. In the bean field the area under the curve are (AUC) are 88.73% for unsupervised data and 94.84% for the supervised data. In the spinach field the area under the curve are (AUC) are 94.34% for unsupervised data and 95.70% for the supervised data. Supervised and unsupervised data means respectively data labeled in supervised and unsupervised way.

Preprints (www.preprints.org) | NOT PEER-REVIEWED | Posted: 5 September 2018 doi:10.20944/preprints201809.0088.v1

Peer-reviewed version available at Remote Sens. 2018, 10, 1690; doi:10.3390/rs10111690

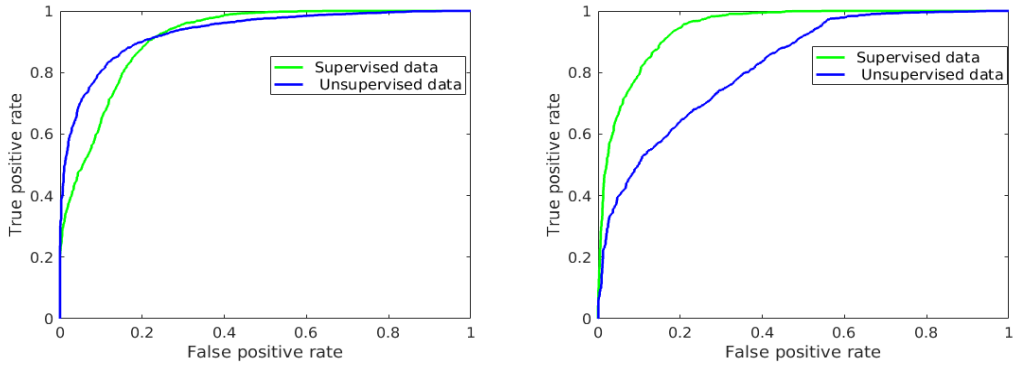

Figure 11. ROC curves of test data with weeds data of the bean field exchanged with that of the spinach field. From left to right the ROC curves computed on the bean (a) and spinach (b) test data. In the bean field the area under the curve are (AUC) are 91.37% for unsupervised data and 93.25% for the supervised data. In the spinach field the area under the curve are (AUC) are 82.70% for unsupervised data and 94.34% for the supervised data. Supervised and unsupervised data means respectively data labeled in supervised and unsupervised way.

Table 4. Results on test data collected in bean field with ResNet18, SVM and Random Forest. For the SVM and RF only the result of the best selected features are presented.

	SVM (AUC%)		**RF (AUC%)**		**ResNet18 (AUC%)**	
Best features	Sup labeling	Unsup labeling	Sup labeling	Unsup labeling	Sup labeling	Unsup labeling
ALL features	**60.60**	44.76	**70.16**	63.95	-	-
Geo3	40.80	**59.51**	48.91	44.86	-	-
Haralick, Color	59.78	40.46	68.15	**65.40**	-	-
-	-	-	-	-	**94.84**	**88.73**

4.2. ResNet vs Features extraction with SVM and RF

SVM and RF have been applied on features extracted on the dataset (Table 1 and Table 2). RF has been performed with 200 trees. As for the Resnet18, models have been created on the data labeled in a supervised and unsupervised way. In order to assess the effectiveness of the selected features we applied them separately and to select the set of features that gives the optimal classification result we mixed them together. In Figure 12 and Figure 13 we have noticed that the color, Haralick and geometric features give the best results. In the field of spinach, the strong presence of thistle with leaves color different from that of spinach at a certain level of growth explain the effectiveness of the color features. In the bean field, the color features were less effective than the texture features (Haralick) in both dataset since we have young potatoes shoots from the previous sowing among the weeds and they have a color almost similar to that of the bean plants.

By Using SVM, while the features are combined, the improvement is less than 2% for data labeled in a supervised manner and about 10% for unsupervised data in the spinach field. In the bean field the same remark applies to the data collected in a supervised manner, for unsupervised data collected no improvement has been found. Another remark that can be made is that from one type of data to another the best features are not the same. We also noticed that the selected features are not suitable to detect the weeds present in the bean field. With the RF, the feature selection procedure only increased performance by about 1% for both spinach dataset. In the bean field an improvement of about 1% have been observed on data labeled in unsupervised way and about 5% for data labeled in supervised way. Table 4 and Table 5 present the result of SVM and RF with best selected features.

Preprints (www.preprints.org) | NOT PEER-REVIEWED | Posted: 5 September 2018 doi:10.20944/preprints201809.0088.v1

Peer-reviewed version available at Remote Sens. 2018, 10, 1690; doi:10.3390/rs10111690

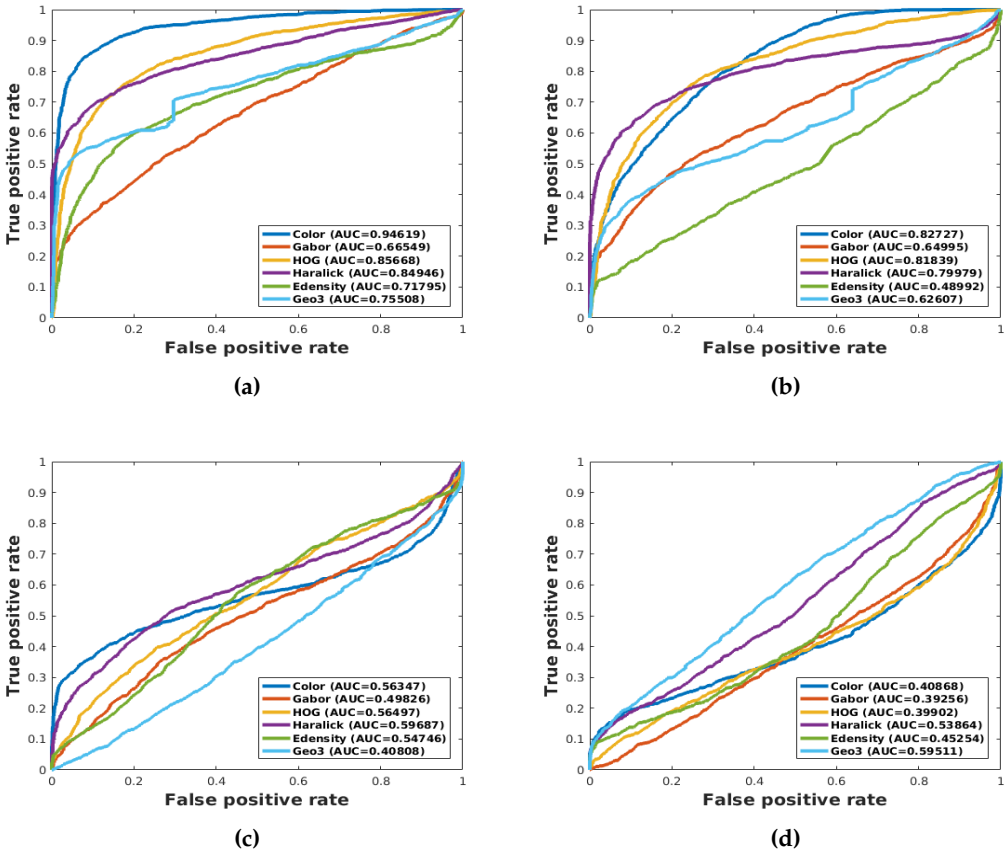

Figure 12. ROC curves of the SVM models created by each features for each field. First line represents the spinach field and the second one the bean field. The first and second column are respectively the training on the the supervised and unsupervised data.

Table 5. Results on test data collected in spinach field with ResNet18, SVM and Random Forest. For the SVM and RF only the result of the best selected features are presented. Sup and Unsup mean respectively supervised and unsupervised.

Best features	SVM (AUC%)		RF (AUC%)		ResNet18 (AUC%)	
	Sup labeling	Unsup labeling	Sup labeling	Unsup labeling	Sup labeling	Unsup labeling
Color, HOG, Gabor	**95.94**	87.38	93.50	95.131	-	-
Haralick, Color, HOG, Gabor	93.93	**90.77**	95.464	**96.177**	-	-
All features	93.352	90.70	**96.99**	95.162	-	-
-	-	-	-	-	**95.70**	**94.34**

Preprints (www.preprints.org) | NOT PEER-REVIEWED | Posted: 5 September 2018 doi:10.20944/preprints201809.0088.v1

Peer-reviewed version available at Remote Sens. 2018, 10, 1690; doi:10.3390/rs10111690

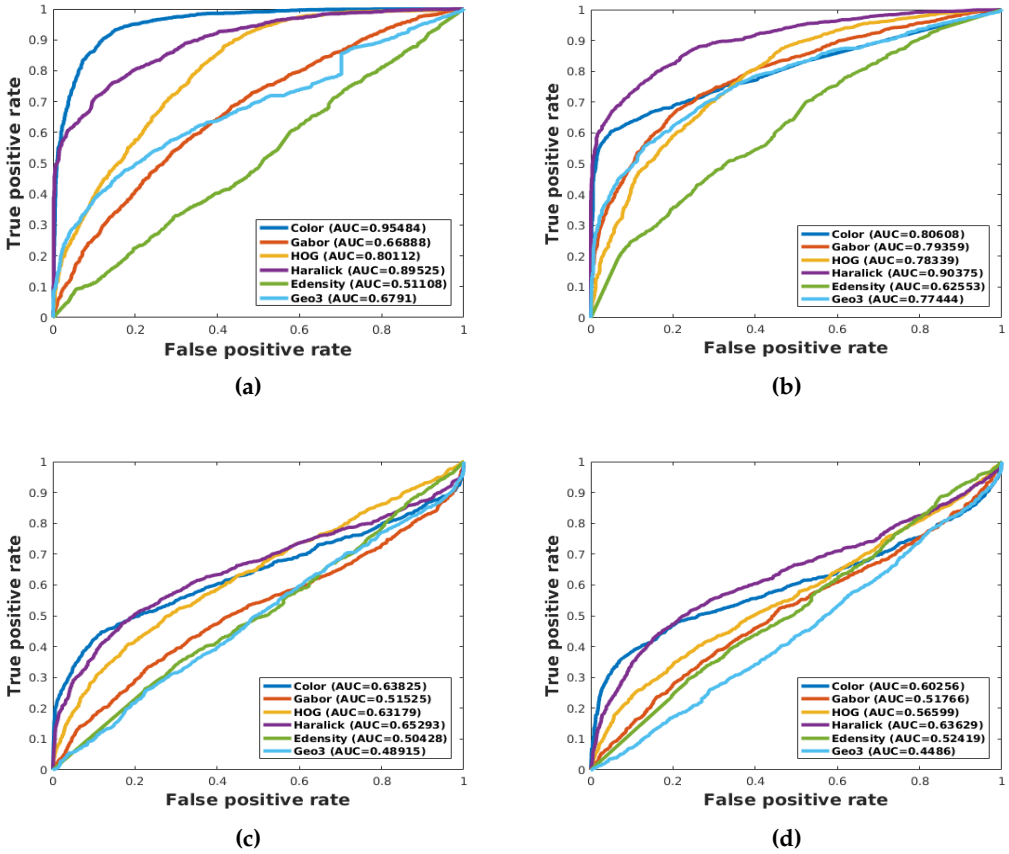

Figure 13. ROC curves of the RF models created by each features for each field. First line represents the spinach field and the second one the bean field. The first and second column are respectively the training on the the supervised and unsupervised data.

In Table 5 we have remarked that ResNet18 provides much better results than SVM and RF in the bean field, with a performance difference greater than 20%. However in the spinach field the results obtained are comparable and sometimes the results of ResNet18 are lower than those of SVM and RF (Table 5). This performance of ResNet18 can be explained by the small amount of data used for the training in the spinach field. For deep learning algorithms the more data we have, the better the algorithm learns. We can also note that the performances of the models formed by the two types of data collected are comparable for the three classification methods. The maximum difference is about 6% in both fields.

Through those results, we can say that even whether we manage to select the most suitable features to identify weeds in a field it is possible that these features are not adapted to another field with a different type of culture. They also show that the features considered better by a classifier can not necessarily be the best if you change classifier. However, in the fields from one year to another there is a possibility to find new types of weeds and that the level of growth of the plants can sometimes cause confusion between weeds and crops, which leads to a new collection of weeds/crop data and a selection of features. Thus for an efficient classification it would be interesting to use a tool capable of automatically generating relevant samples and features to detect weeds, hence the interest of using deep learning with unsupervised data labeling.

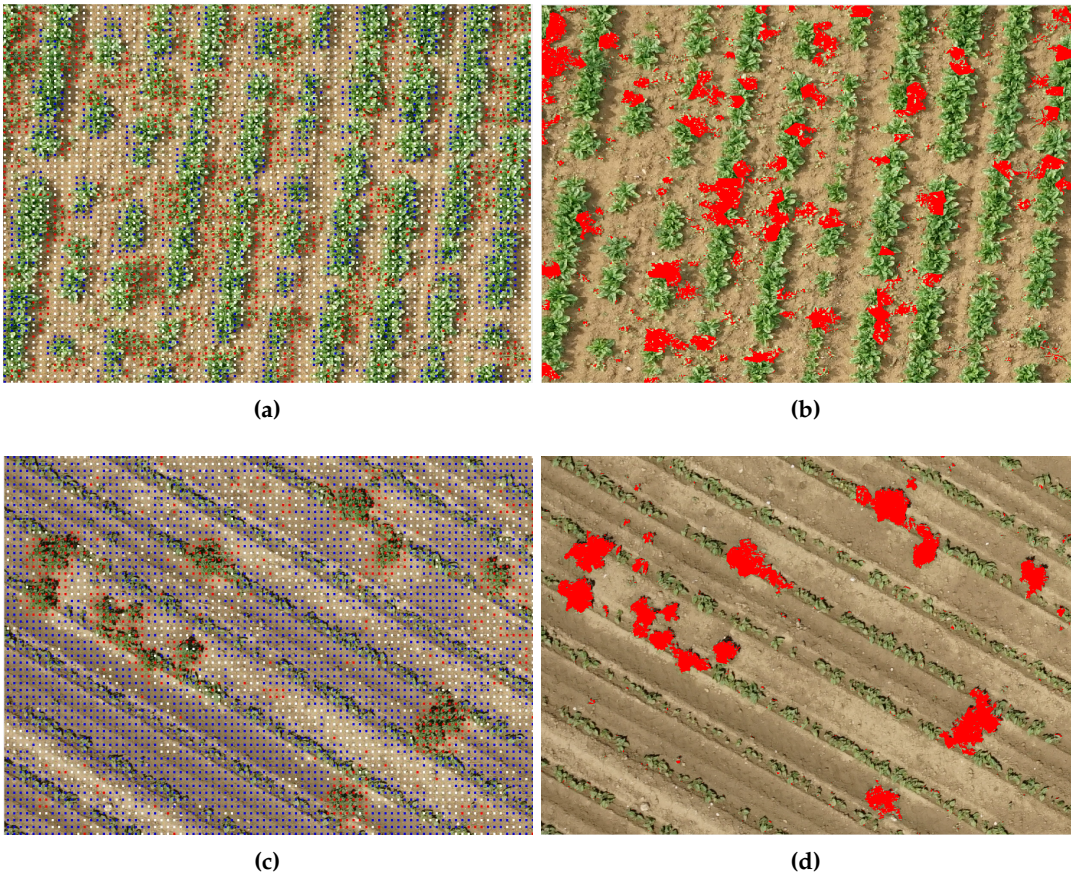

Figure 14. Example of UAV image classification with models created by unsupervised data in two different fields. From first to the second line we have samples from spinach and bean fields. On the first column we have the samples obtained after using sliding window, without crop lines and background information. Blue, red and white dot mean that the plants are is identified as weed, crop and uncertain decision respectively. On the second column we have the detected weeds in red after crop lines and background information have been applied.

4.3. Weeds detection

In the aim to detect weeds in entire UAV image we applied an overlapping window for weeds detection. For each position of the window the CNNs models provide the probability of being weeds or crops. Thus, the center of the extracted image is marked by a colored dot according to the probabilities. Blue, red and white dot mean respectively that the extracted image is identified as weed, crop and uncertain decision (Figures 14a and 14c). Uncertain decision means the both probabilities are very close to 0.5. Thereafter, we used crop lines information and superpixels that have been created before, to classify all the pixels of the image. On each superpixel we look which color of dot has the majority. A superpixel is classed as crop or weed if the most represented dots are in blue respectively in red. For superpixels that have white dots as majority we used crop lines information. Hence, superpixels which are in the crop lines are regarded as crop and the others are weeds. The superpixels created in the background are removed. Figures 14b and 14d present the classification results in parts of spinach and bean fields. On those figures we remark that interline weeds and intra-line weeds have been detected with a low overdetection. Overdetections are mainly found on the edges of the crop rows where the window cannot overlap the whole plant. Some pixels of weeds are not entirely in red, because after performing the threshold on the ExG, the parts of these plants which are less green are considered as soil.

However, the unsupervised data collection method depends strongly on the efficiency of the crop line detection method and also the presence of weeds in the interline. The line detection approach used here has already shown its effectiveness in beet and corn fields in our previous work [43]. With the bean field we found even if a field does not have a lot of samples of weeds in the interline it is possible to create a robust model with data-augmentation. We also noticed using a deep learning architecture such as ResNet18 we can create robust models for classification of weeds in bean or spinach fields with supervised or unsupervised data annotation. The main advantage of our method is that it is fully automatic.

5. Conclusion

In this paper, we proposed a novel fully automatic learning method using Convolutional Neuronal Networks CNNs) with unsupervised training dataset collection for weeds detection from UAV images taken in bean and spinach fields. The results obtained have shown close performance to the supervised data labeling ones. The Area Under Curve (AUC) differences are 1.5% in the spinach field and 6% in the bean field. Supervised labeling is an expensive task for human experts and according to the gaps of accuracies between the supervised and the unsupervised labeling, our method can be a better choice in the detection of weeds, especially when the crop rows are spaced. The proposed method is interesting in terms of flexibility and adaptivity, since the models can be easily trained in new dataset. We also found that ResNet18 architecture can extract useful features for classification of weeds in bean or spinach fields with data labeled with supervised or unsupervised way. In addition the developed method could be a key of online weeds detection with UAV. As future work we plan to use multispectral images because in some conditions near infra red could help to distinguish plant even if they have a similarity in the visible spectral and leave shape. With the near infra-red we plan also to improve the background segmentation.

Funding: This work is part of the ADVENTICES project supported by the Centre-Val de Loire Region (France), grant number ADVENTICES 16032PR.

Author Contributions: M.D.B., A.H. and R.C. conceived and designed the method; M.D.B implemented the method and performed the experiments; M.D.B., A.H. and R.C. wrote the paper, discussed the results and revised the manuscript. All authors have read and approved the manuscript.

Conflicts of Interest: The authors declare no conflict of interest.

References

1. European Crop Protection. With or without pesticides? | ECPA, 2017.
2. Oerke, E.C. Crop losses to pests. *The Journal of Agricultural Science* **2006**, *144*, 31. doi:10.1017/S0021859605005708.
3. Pierce, F.J.; Nowak, P. Aspects of Precision Agriculture; 1999; pp. 1–85. doi:10.1016/S0065-2113(08)60513-1.
4. McBratney, A.; Whelan, B.; Ancev, T.; Bouma, J. Future Directions of Precision Agriculture. *Precision Agriculture* **2005**, *6*, 7–23. doi:10.1007/s11119-005-0681-8.
5. Torres-Sánchez, J.; López-Granados, F.; Peña, J.M. An automatic object-based method for optimal thresholding in UAV images: Application for vegetation detection in herbaceous crops. *Computers and Electronics in Agriculture* **2015**, *114*, 43–52. doi:10.1016/j.compag.2015.03.019.
6. Zhang, C.; Kovacs, J.M. The application of small unmanned aerial systems for precision agriculture: a review. *Precision Agriculture* **2012**, *13*, 693–712. doi:10.1007/s11119-012-9274-5.
7. Dos Santos Ferreira, A.; Matte Freitas, D.; Gonçalves da Silva, G.; Pistori, H.; Theophilo Folhes, M. Weed detection in soybean crops using ConvNets. *Computers and Electronics in Agriculture* **2017**, *143*, 314–324. doi:10.1016/j.compag.2017.10.027.
8. Bah, M.D.; Dericquebourg, E.; Hafiane, A.; Canals, R. Deep learning based classification system for identifying weeds using high-resolution UAV imagery. Computing Conference 2018, 2018.
9. Hamuda, E.; Glavin, M.; Jones, E. A survey of image processing techniques for plant extraction and segmentation in the field. *Computers and Electronics in Agriculture* **2016**, *125*, 184–199. doi:10.1016/j.compag.2016.04.024.

10. Gée, C.; Bossu, J.; Jones, G.; Truchetet, F. Crop/weed discrimination in perspective agronomic images. *Computers and Electronics in Agriculture* **2008**, *60*, 49–59. doi:10.1016/j.compag.2007.06.003.
11. Woebbecke, D.; Meyer, G.; Von Bargen, K.; Mortensen, D. Color indices for weed identification under various soil, residue, and lighting conditions. *Transactions of the ASAE* **1995**, *38*, 259–269. doi:10.13031/2013.27838.
12. Otsu, N. A threshold selection method from gray-level histograms. *IEEE Transactions on Systems, Man, and Cybernetics* **1979**, *9*, 62–66. doi:10.1109/TSMC.1979.4310076.
13. Hough, P.V.C. Method and means for recognizing complex patterns. *US Patent 3,069,654* **1962**, *21*, 225–231. doi:10.1007/s10811-008-9353-1.
14. Peña, J.M.; Torres-Sánchez, J.; Isabel De Castro, A.; Kelly, M.; López-Granados, F. Weed Mapping in Early-Season Maize Fields Using Object-Based Analysis of Unmanned Aerial Vehicle (UAV) Images. *PLoS ONE* **2013**, *8*. doi:10.1371/journal.pone.0077151.
15. Blaschke, T. Object based image analysis for remote sensing. *ISPRS Journal of Photogrammetry and Remote Sensing* **2010**, *65*, 2–16. doi:10.1016/J.ISPRSJPRS.2009.06.004.
16. Tang, L.; Tian, L.; Steward, B.L. Classification of Broadleaf and Grass Weeds Using Gabor Wavelets and an Artificial Neural Network. *Transactions of the American Society of Agricultural Engineers* **2003**, *46*, 1247–1254.
17. Jeon, H.Y.; Tian, L.F.; Zhu, H. Robust crop and weed segmentation under uncontrolled outdoor illumination. *Sensors* **2011**, *11*, 6270–6283. doi:10.3390/s110606270.
18. Ahmed, F.; Al-Mamun, H.A.; Bari, A.S.M.H.; Hossain, E.; Kwan, P. Classification of crops and weeds from digital images: A support vector machine approach. *Crop Protection* **2012**, *40*, 98–104. doi:10.1016/j.cropro.2012.04.024.
19. Latha, M.; Poojith, A.; Reddy, A.; Kumar, V. Image Processing in Agriculture. *International Journal Of Innovative Research In Electrical, Electronics, Instrumentation And Control Engineering* **2014**, *2*, 2321–2004.
20. Pérez-Ortiz, M.; Peña, J.M.; Gutiérrez, P.A.; Torres-Sánchez, J.; Hervás-Martínez, C.; López-Granados, F. Selecting patterns and features for between- and within- crop-row weed mapping using UAV-imagery. *Expert Systems With Applications* **2015**, *47*, 85–94, [ESWA 10373]. doi:10.1016/j.eswa.2015.10.043.
21. Bakhshipour, A.; Jafari, A.; Nassiri, S.M.; Zare, D. Weed segmentation using texture features extracted from wavelet sub-images. *Biosystems Engineering* **2017**, *157*, 1–12. doi:10.1016/j.biosystemseng.2017.02.002.
22. Bakhshipour, A.; Jafari, A. Evaluation of support vector machine and artificial neural networks in weed detection using shape features. *Computers and Electronics in Agriculture* **2018**, *145*, 153–160. doi:10.1016/J.COMPAG.2017.12.032.
23. Gao, J.; Liao, W.; Nuyttens, D.; Lootens, P.; Vangeyte, J.; Pižurica, A.; He, Y.; Pieters, J.G. Fusion of pixel and object-based features for weed mapping using unmanned aerial vehicle imagery. *International Journal of Applied Earth Observation and Geoinformation* **2018**, *67*, 43–53. doi:10.1016/j.jag.2017.12.012.
24. LeCun, Y.; Bottou, L.; Bengio, Y.; Haffner, P. Gradient-based learning applied to document recognition. *Proceedings of the IEEE* **1998**, *86*, 2278–2323, [1102.0183]. doi:10.1109/5.726791.
25. Krizhevsky, A.; Sutskever, I.; Hinton, G.E. ImageNet Classification with Deep Convolutional Neural Networks. *Advances In Neural Information Processing Systems* **2012**, pp. 1–9, [1102.0183]. doi:http://dx.doi.org/10.1016/j.protcy.2014.09.007.
26. Hung, C.; Xu, Z.; Sukkarieh, S. Feature Learning Based Approach for Weed Classification Using High Resolution Aerial Images from a Digital Camera Mounted on a UAV. *Remote Sensing* **2014**, *6*, 12037–12054. doi:10.3390/rs61212037.
27. Mortensen, A.K.; Dyrmann, M.; Karstoft, H.; Nyholm Jørgensen, R.; Gislum, R. Semantic Segmentation of Mixed Crops using Deep Convolutional Neural Network. CIGR-AgEng conference, 2016.
28. Milioto, A.; Lottes, P.; Stachniss, C. Real-time blob-wise sugar beets vs weeds classification for monitoring fields using convolutional neural networks. *ISPRS Annals of Photogrammetry, Remote Sensing and Spatial Information Sciences* **2017**, *IV-2/W3*, 41–48. doi:10.5194/isprs-annals-IV-2-W3-41-2017.
29. Di Cicco, M.; Potena, C.; Grisetti, G.; Pretto, A. Automatic model based dataset generation for fast and accurate crop and weeds detection. 2017 IEEE/RSJ International Conference on Intelligent Robots and Systems (IROS). IEEE, 2017, pp. 5188–5195. doi:10.1109/IROS.2017.8206408.
30. Louargant, M.; Jones, G.; Faroux, R.; Paoli, J.N.; Maillot, T.; Gée, C.; Villette, S. Unsupervised Classification Algorithm for Early Weed Detection in Row-Crops by Combining Spatial and Spectral Information. *Remote Sensing* **2018**, *10*, 761. doi:10.3390/rs10050761.

31. Jones, G.; Gée, C.; Truchetet, F. Modelling agronomic images for weed detection and comparison of crop/weed discrimination algorithm performance. *Precision Agriculture* **2009**, *10*, 1–15. doi:10.1007/s11119-008-9086-9.
32. Montalvo, M.; Pajares, G.; Guerrero, J.M.; Romeo, J.; Guijarro, M.; Ribeiro, A.; Ruz, J.J.; Cruz, J.M. Automatic detection of crop rows in maize fields with high weeds pressure. *Expert Systems With Applications* **2012**, *39*, 11889–11897. doi:10.1016/j.eswa.2012.02.117.
33. Achanta, R.; Shaji, A.; Smith, K.; Lucchi, A.; Fua, P.; Süsstrunk, S. SLIC Superpixels Compared to State-of-the-Art Superpixel Methods. *Pattern Analysis and Machine Intelligence, IEEE Transactions on* **2011**, *34*, 2274–2282. doi:10.1109/tpami.2012.120.
34. Kamilaris, A.; Prenafeta-Boldú, F.X. Deep learning in agriculture: A survey. *Computers and Electronics in Agriculture* **2018**, *147*, 70–90. doi:10.1016/J.COMPAG.2018.02.016.
35. He, K.; Zhang, X.; Ren, S.; Sun, J. Deep Residual Learning for Image Recognition. 2016 IEEE Conference on Computer Vision and Pattern Recognition (CVPR). IEEE, 2016, pp. 770–778. doi:10.1109/CVPR.2016.90.
36. Simonyan, K.; Zisserman, A. Very Deep Convolutional Networks for Large-Scale Image Recognition. *arXiv preprint arXiv:1409.1556* **2015**, pp. 1–14, [arXiv:1409.1556v6]. doi:10.1016/j.infsof.2008.09.005.
37. Lottes, P.; Khanna, R.; Pfeifer, J.; Siegwart, R.; Stachniss, C. UAV-based crop and weed classification for smart farming. 2017 IEEE International Conference on Robotics and Automation (ICRA). IEEE, 2017, pp. 3024–3031. doi:10.1109/ICRA.2017.7989347.
38. Dalal, N.; Triggs, W.; Triggs, B. Histograms of Oriented Gradients for Human Detection, 2004, [arXiv:chao-dyn/9411012]. doi:10.1109/CVPR.2005.177.
39. Xiao, X.Y.; Hu, R.; Zhang, S.W.; Wang, X.F. HOG-based approach for leaf classification. Advanced Intelligent Computing Theories and Applications. With Aspects of Artificial Intelligence: 6th International Conference on Intelligent Computing, ICIC 2010, Changsha, China, August 18-21, 2010. Proceedings. Springer, Berlin, Heidelberg, 2010, Vol. 6216 LNAI, pp. 149–155. doi:10.1007/978-3-642-14932-0_19.
40. Haralick, R.M.; Shanmugam, K. Textural Features for Image Classification. *Systems, Man and Cybernetics* **1973**, *3*, 610 – 621. doi:10.1109/TSMC.1973.4309314.
41. Agrawal, K.N.; Singh, K.; Bora, G.C.; Lin, D. Weed Recognition Using Image-Processing Technique Based on Leaf Parameters. *Journal of Agricultural Science and Technology B Journal of Agricultural Science and Technology* **2012**, *2*, 1939–1250.
42. de Castro, A.I.; Torres-Sánchez, J.; Peña, J.M.; Jiménez-Brenes, F.M.; Csillik, O.; López-Granados, F. An automatic random forest-OBIA algorithm for early weed mapping between and within crop rows using UAV imagery. *Remote Sensing* **2018**, *10*, 1–21. doi:10.3390/rs10020285.
43. Bah, M.D.; Hafiane, A.; Canals, R. Weeds detection in UAV imagery using SLIC and the hough transform. 2017 Seventh International Conference on Image Processing Theory, Tools and Applications (IPTA). IEEE, 2017, pp. 1–6. doi:10.1109/IPTA.2017.8310102.